SLAC-PUB-14514

$LaVO_4$:Eu Phosphor Films with Enhanced Eu Solubility

T. Higuchi,[1,*] Y. Hotta,[1] Y. Hikita,[1] S. Maruyama,[2] Y. Hayamizu,[2] H. Akiyama,[2] H. Wadati,[3] D. G. Hawthorn,[3] T. Z. Regier,[4] R. I. R. Blyth,[4] G. A. Sawatzky,[3] and H. Y. Hwang[1,5,6]

[1] *Department of Advanced Materials Science, University of Tokyo, Kashiwa, Chiba 277-8561, Japan*
[2] *Institute for Solid State Physics, University of Tokyo, Kashiwa, Chiba 277-8581, Japan*
[3] *Department of Physics and Astronomy, University of British Columbia, Vancouver, British Columbia V6T 1Z1, Canada*
[4] *Canadian Light Source, University of Saskatchewan, Saskatoon, Saskatchewan S7N 0X4, Canada*
[5] *Japan Science and Technology Agency, Kawaguchi, 332-0012, Japan*
[6] *Department of Applied Physics and Stanford Institute for Materials and Energy Science, Stanford University, Stanford, CA 94305, USA*

(Dated: January 6, 2011)

Eu doped rare-earth orthovanadates are known to be good red phosphor materials. In particular, $LaVO_4$:Eu is a promising candidate due to the low Eu-site point symmetry, and thus high dipole transition probability within Judd-Ofelt theory. However, the low solubility limit (< 3 mol%) of Eu in $LaVO_4$ prevents its efficient use as a phosphor. We present optical evidence of enhanced Eu solubility as high as 10 mol% in $LaVO_4$:Eu thin films grown by pulsed laser deposition and postannealing. The photoluminescent intensity exceeded that of YVO_4:Eu thin films when excited below the host bandgap, indicating stronger direct emission of Eu in $LaVO_4$.

PACS numbers: 68.35.-p, 78.66.-w, 78.70.Dm

Rare-earth (R) orthovanadates RVO_4 have been of particular interest due to their unique properties and wide applications such as phosphors [1], laser host materials [2, 3], solar cells [4], and amplifiers for fiber-optic communication [5]. RVO_4:Eu is known as an excellent phosphor with bright red emission [1]. This red luminescence mainly corresponds to the transitions of the Eu $4f$ multiplet states, from the $^5D_0$ level to the ^7F_J states (J = 0 to 5), which are normally dipole prohibited. In materials, however, dipole transitions are allowed by the perturbation via crystal fields with odd parity, as described by Judd-Ofelt theory [6, 7]. In RVO_4:Eu, the Eu substitutes the R site because of their matched valence and size. Its point symmetry depends on the host crystal structure, and the ionic radii of the R element determines the crystal structure of orthovanadates.

$LaVO_4$ usually forms in the monazite structure with a space group of $P2_1/c$ due to the large ionic radii of La [8], and is a promising candidate as a host material for Eu doping due to the low point symmetry (C_1) around the R site. However, the poor solubility limit of Eu (< 3 mol%) has prevented its effectiveness. Moreover, the large spacing between the Eu ions and VO_4 tetrahedrons in $LaVO_4$ reduces overlap of their wave functions, resulting in reduced indirect emission via energy transfer from the host material to the activators. On the other hand, reflecting the smaller radii of Y^{3+} and Eu^{3+}, YVO_4 and $EuVO_4$ has the closer packed zircon structure with space group $I4_1/amd$, achieving complete solubility of Eu in YVO_4 [9]. Therefore, $LaVO_4$:Eu is surpassed as a phosphor by YVO_4:Eu, which is currently used commercially with a quantum yield as high as 70 % [1].

Efforts to improve the luminescent properties of $LaVO_4$:Eu have been made by changing its crystal structure. Meta-stable zircon $LaVO_4$ was synthesized via hydrothermal process under high pressure [10] or controlled pH [11], and enhanced luminescent properties of $LaVO_4$:Eu was achieved in zircon nano-crystals [11, 12]. In this Letter, we present optical evidence of a different meta-stable structure of $LaVO_4$:Eu. The conventional Eu solubility limit in monazite $LaVO_4$ can be exceeded by growing first a perovskite solid solution of $LaVO_3$ and $EuVO_3$ by pulsed laser deposition (PLD), and gently postannealing it to convert to $LaVO_4$:Eu. The lower symmetry around the Eu site in monazite $LaVO_4$ enhanced the direct absorption by Eu, resulting in stronger photoluminescence (PL) than that of YVO_4:Eu when excited by photons below the host bandgap.

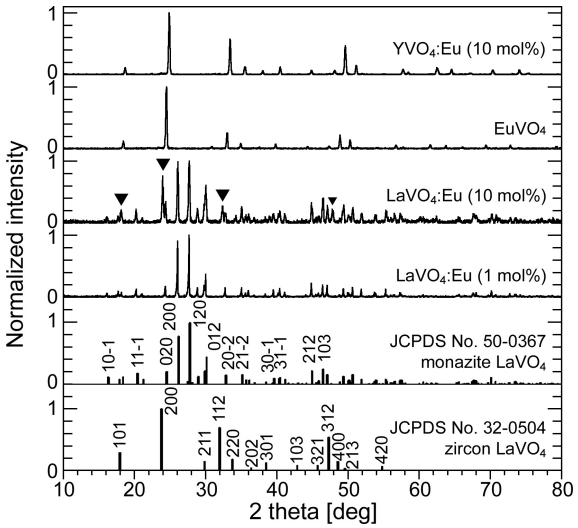

FIG. 1: Powder XRD patterns of the polycrystalline pellets. Reference patterns of the monazite and zircon type $LaVO_4$ are also plotted. Triangles indicate the peaks corresponding to the zircon phase in $LaVO_4$:Eu (10 %).

RVO_4 films were grown via conversion of an epitaxial perovskite $RVO_3/SrTiO_3$ heterostructure by postannealing in oxygen. Four polycrystalline PLD targets, $LaVO_4$:Eu (1 mol%), $LaVO_4$:Eu (10 mol%), YVO_4:Eu (10 mol%), and $EuVO_4$, were synthesized from La_2O_3, Y_2O_3, Eu_2O_3, and V_2O_5 through solid state reaction synthesis. The crystal structure of the pellets was determined by powder x-ray diffraction (XRD), as shown in Fig. 1. $LaVO_4$:Eu (1 mol%) was a single phase with the monazite structure, while $LaVO_4$:Eu (10 mol%) showed additional peaks. These extra peaks could be indexed to zircon $EuVO_4$, reflecting genera-

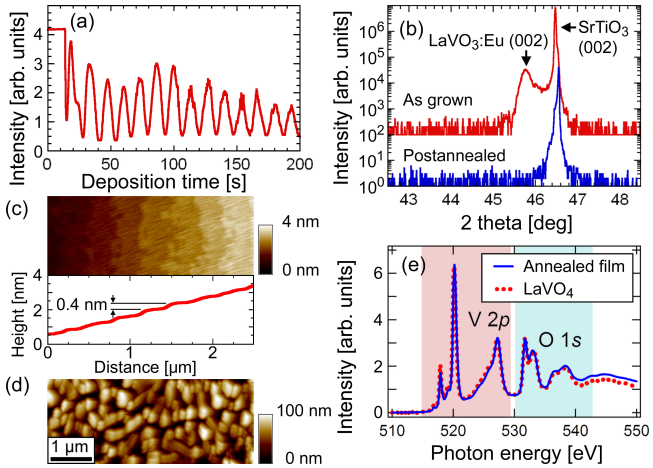

FIG. 2: (Color online) (a) Typical RHEED oscillations during growth of RVO$_3$ films. (b) XRD θ-2θ scan of the as-grown LaVO$_3$:Eu (10 mol%) film and after annealing. The Miller indices are labeled in a manner following the cubic crystal structure of the SrTiO$_3$ substrate. AFM topography of the LaVO$_x$:Eu (10 mol%) film (c) as-grown and (d) after postannealing. (e) XAS spectra of the postannealed LaVO$_4$ film. Reference spectrum of LaVO$_4$ was taken from Ref. [13].

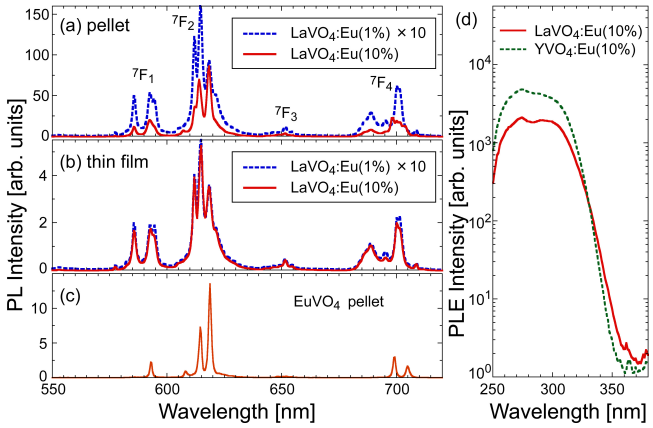

FIG. 3: (Color online) PL spectra of (a) the polycrystalline pellets and (b) the postannealed films of LaVO$_4$:Eu and (c) the EuVO$_4$ pellet. (d) PLE spectra obtained from the postannealed LaVO$_4$:Eu (10 mol%) and YVO$_4$:Eu (10 mol%) films. Note that YVO$_4$:Eu (10 mol%) and EuVO$_4$ showed a similar PL shape, reflecting the same zircon structure of the host material, independent of whether they are pellets or films (data not shown).

tion of secondary phases due to the excess Eu above its bulk solubility limit in LaVO$_4$. Note the zircon peak positions in LaVO$_4$:Eu (10 mol%) were observed at slightly smaller angle than EuVO$_4$, which suggests this phase-separated zircon phase was not pure EuVO$_4$, but La$_{1-x}$Eu$_x$VO$_4$ with sufficient Eu concentration to stabilize the zircon phase.

40 nm thick RVO$_3$ films were grown on SrTiO$_3$ (001) substrates by PLD, using a KrF excimer laser with a laser fluence of 1.0 J/cm^2, a spot size of 1.6 mm^2, and repetition rate of 8 Hz. When films of RVO$_x$ are grown by PLD, their structure is very sensitive to thermodynamic conditions. The growth phase diagram of LaVO$_x$ by PLD has been extensively studied, and selective growth of LaVO$_3$ and LaVO$_4$ was achieved by controlling the oxygen partial pressure(P_{O_2}) and substrate temperature (T_{sub}) during growth [14]. The thermodynamic condition to stabilize V^{3+} or V^{5+} is expected to be similar in RVO$_x$, since the valence state of R is fixed to be trivalent, and the variable valence is that of V in these compounds [15–17]. Therefore, the same growth conditions as used for LaVO$_3$ were used to grow single phase perovskite RVO$_3$. The substrates were preannealed at T_{sub} = 950 °C and P_{O_2} = 5 × 10^{-6} Torr for 30 minutes, and during deposition, T_{sub} = 600 °C and P_{O_2} = 5 × 10^{-7} Torr. Clear reflection high-energy electron diffraction (RHEED) oscillations corresponding to two-dimensional unit cell growth were observed during growth of RVO$_3$, and the thickness of the layers was monitored by the oscillations in the growth [Fig. 2(a)]. The lattice constant (c = 3.96 Å) of the film measured by the X-ray diffraction (XRD) θ-2θ scan [Fig. 2(b)] was slightly larger than the pseudocubic lattice constant (3.93 Å) of the bulk [18] because of the compressive strain from the substrate.

The as-grown films grown by PLD were then postannealed at 600 °C in oxygen flow for 24 hours to convert the structure to RVO$_4$. As shown in Fig. 2(b), the peak in the XRD scan corresponding to perovskite RVO$_3$ disappeared after postannealing. The absence of the peaks from RVO$_4$ is likely due to the small grain size and total volume. The conversion of the films was also studied by atomic force microscopy (AFM) [Figs. 2(c) and (d)], and the postannealing changed the surface topography completely. The as-grown RVO$_3$ films showed the perovskite step-and-terrace structures with step height of ∼ 4 nm, reflecting the slight miscut angle of the substrate, while the annealed samples showed granular surfaces.

The structural conversion of the host material, LaVO$_x$, was also examined by X-ray absorption spectroscopy (XAS) measured in total-electron-yield mode as shown in Fig. 2(e). X-ray absorption experiments were performed at beamline 11ID-1 (SGM) of the Canadian Light Source. The V 2p and O 1s core-level spectra are very sensitive to the V valence states. The sharp features of the XAS spectrum obtained from the postannealed film is characteristic of V^{5+} in LaVO$_4$, and was almost identical to that of the reference XAS spectrum for LaVO$_4$ [13]. By postannealing in oxygen, the valence state of V was expected to change from V^{3+} in RVO$_3$ to V^{5+} in RVO$_4$, and the observation of valence change by XAS indicated that the structural conversion was completed in the annealed film, which could not be determined by XRD structural assignment due to the small coherent volume of the film.

The PL of the polycrystalline pellets and the annealed thin films was measured under excitation by the fourth-harmonic of a Nd:YVO$_4$ laser with a wavelength (λ) of 266 nm, as shown in Figs. 3 (a) and (b). The fluorescence spectra of Eu^{3+} ions, especially the splitting and the intensity ratio of the peaks, are very sensitive to the local structure around it in the material. As examined by XRD, polycrystalline LaVO$_4$:Eu (1 mol%) consisted of single phase monazite, and its PL spectra can be used as a reference. The shape of PL from LaVO$_4$:Eu (10 mol%) can be well fitted by a linear combination of the LaVO$_4$:Eu (1 mol%) and the zircon EuVO$_4$ [Fig. 3(c)] spectra. This is consistent with the structural study by XRD, which indicates that polycrystalline LaVO$_4$:Eu (10 mol%) has two separated phases with

the zircon and monazite structures, and Eu is distributed to both phases.

Unlike that of the polycrystalline pellet, the spectrum of the $LaVO_4$:Eu (10 mol%) film showed almost identical features to that of the $LaVO_4$:Eu (1 mol%) reference. Moreover, the PL intensity was almost ten times as large as that of the $LaVO_4$:Eu (1 mol%) film — it is proportional to the total number of Eu^{3+} ions, which is a noteworthy difference from the case of the phase-separated bulk pellet, where the PL intensity was smaller than expected from the increase of activator ions. Since Eu substitutes at the La site in $LaVO_4$:Eu (1 mol%) with a single monazite phase, this correspondence of the PL profile and intensity indicates that the 10 mol% of Eu is fully incorporated at the La site in the monazite $LaVO_4$ films. Segregation of Eu in other forms, for example Eu_2O_3 was unlikely, because they have PL features different from that of monazite $LaVO_4$:Eu. In addition, within the possible chemical compounds, Eu^{3+} can only be deactivated in V compounds with V $3d$ electrons due to their excitation energy below that of Eu^{3+}, which was ruled out by XAS. Therefore, segregated phases incorporating dark Eu could be excluded.

It is striking that $LaVO_4$:Eu (10 mol%) consisted of a single monazite phase in the PLD grown films, even though the Eu concentration exceeded the bulk solubility in $LaVO_4$. $LaVO_3$ and $EuVO_3$ have the same perovskite structure [19], resulting in complete solubility in the epitaxial structures, and moderate annealing at a temperature far lower than the melting point does not induce significant migration of atoms. Another aspect of the lack of phase separation is the small volume of the films. Crystal phase separation kinetics often depends on the crystal size [11, 20], and in thin films phase separation can be suppressed, because the energy gain by phase separation is small compared to the large grains obtained by bulk solid state reaction.

To study the excitation mechanism of the activator ions, the photoluminescence excitation (PLE) spectra were recorded from the annealed $LaVO_4$:Eu (10 mol%) and YVO_4:Eu (10 mol%) films, using a grating monochrometer with a Xe lamp for the excitation ([Fig. 3(c)]). The $LaVO_4$:Eu (10 mol%) film showed a larger tail of PLE spectra below the bandgap. This can be understood based on the difference between the direct excitation of the activators, and the indirect process via energy transfer from the excited host material [1, 21]. When they are excited by light with energy higher than the bandgap, 3.8 eV ($\lambda = 326$ nm) in $LaVO_4$ and 3.7 eV ($\lambda = 335$ nm) in YVO_4 [22], due to the stronger energy transfer from VO_4 to Eu, YVO_4 shows stronger PL, which was indeed observed when excited by $\lambda = 266$ nm light. If the excitation photon energy is smaller than the host bandgap, however, the optical penetration depth in the host material is much larger than the film thickness (40 nm) and the indirect process is suppressed. Therefore, the $LaVO_4$:Eu films showed stronger emission due to its direct excitation process in this regime.

In summary, structural conversion of PLD-grown RVO_3 epitaxial thin films to RVO_4 by postannealing was confirmed. Using this technique, phosphor RVO_4:Eu films were fabricated. The PL spectrum of the $LaVO_4$:Eu (10 mol%) thin films showed identical shape as that of the 1 mol% doped film and its intensity was proportional to the Eu doping concentration, indicating the enhancement of the solid solubility limit of Eu in the films up to as high as 10 mol%. Especially when excited by photons below the bandgap, the PL intensity exceeded that of the YVO_4:Eu (10 mol%) with the same thickness, reflecting the stronger direct emission of Eu via dipole transitions. Epitaxial growth of RVO_3 perovskite films before postannealing played a key role in the structural control, by prefixing the substituting site in fully incorporated structures, and this technique may provide a general approach for enhancing phosphor films.

The authors appreciate L. Fitting-Kourkoutis and D. A. Muller for helpful discussions. H. Y. H. acknowledges support from the Department of Energy, Office of Basic Energy Sciences, Division of Materials Sciences and Engineering, under contract DE - AC02 - 76SF00515. The XAS measurements described in this paper were performed at the Canadian Light Source, which is supported by NSERC, NRC, CIHR, and the University of Saskatchewan.

* E-mail: higuchi@ap4.t.u-tokyo.ac.jp

[1] W. L. Wanmaker, A. Bril, J. W. ter Vrugt, and J. Broos, Philips Res. Rep. **21**, 270 (1966).
[2] J. R. O'Connor, Appl. Phys. Lett. **9**, 407 (1966).
[3] R. A. Fields, M. Birnbaum, and C. L. Fincher, Appl. Phys. Lett. **51**, 1885 (1987).
[4] J. Liu, Q. Yao, and Y. Li, Appl. Phys. Lett. **88**, 173119 (2006).
[5] D. B. Barber, C. R. Pollock, L. L. Beecroft, and C. K. Ober, Opt. Lett. **22**, 1247 (1997).
[6] B. R. Judd, Phys. Rev **127**, 750 (1962).
[7] G. S. Ofelt, J. Chem. Phys. **37**, 511 (1962).
[8] J. Bashir and M. Nasir Khan, Mater. Lett. **60**, 470 (2006).
[9] B. C. Chakoumakos, M. M. Abraham, and L. A. Boatner, J. Solid State Chem. **109**, 197 (1994).
[10] Y. Oka, T. Yao, and N. Yamamoto, J. Solid State Chem. **152**, 486 (2000).
[11] W. Fan, Y. Bu, X. Song, S. Sun, and X. Zhao, Cryst. Growth Des. **7**, 2361 (2007).
[12] C. J. Jia, L. D. Sun, F. Luo, X. C. Jiang, L. H. Wei, and C. H. Yan, Appl. Phys. Lett. **84**, 5305 (2004).
[13] H. Wadati, D. G. Hawthorn, J. Geck, T. Z. Regier, R. I. R. Blyth, T. Higuchi, Y. Hotta, Y. Hikita, H. Y. Hwang, and G. A. Sawatzky, Appl. Phys. Lett. **95**, 023115 (2009).
[14] Y. Hotta, Y. Mukunoki, T. Susaki, H. Y. Hwang, L. Fitting, and D. A. Muller, Appl. Phys. Lett. **89**, 031918 (2006).
[15] D. R. Gaskell, *Introduction to the thermodynamics of materials, 4th ed.* (Taylor and Francis, New York, 2003).
[16] L. Fitting Kourkoutis, Y. Hotta, T. Susaki, H. Y. Hwang, and D. A. Muller, Phys. Rev. Lett. **97**, 256803 (2006).
[17] H. Wadati, Y. Hotta, M. Takizawa, A. Fujimori, T. Susaki, and H. Y. Hwang, J. Appl. Phys. **102**, 053707 (2007).
[18] P. Bordet, C. Chaillout, M. Marezio, Q. Huang, A. Santoro, S.-W. Cheong, H. Takagi, C. S. Oglesby, and B. Batlogg, J. Solid State Chem. **106**, 253 (1993).
[19] G. J. McCarthy, C. A. Sipe, and K. E. McIlvried, Mater. Res. Bull. **9**, 1279 (1974).
[20] B. R. Pamplin, *Crystal growth, 2nd ed. (International series on the science of the solid state ; v. 16)* (Pergamon, Oxford ; New York, 1980).
[21] M. Yu, J. Lin, and S. B. Wang, Appl. Phys. A **80**, 353 (2005).
[22] J. D. Kingsley and G. W. Ludwig, J. Appl. Phys. **41**, 370 (1970).